Charles University in Prague
Faculty of Mathematics and Physics
Department of Geophysics

Abstract of the Doctoral Thesis

Numerical modeling of ice sheet dynamics

Ondřej Souček

Supervisor: prof. RNDr. **Zdeněk Martinec**, DrSc.

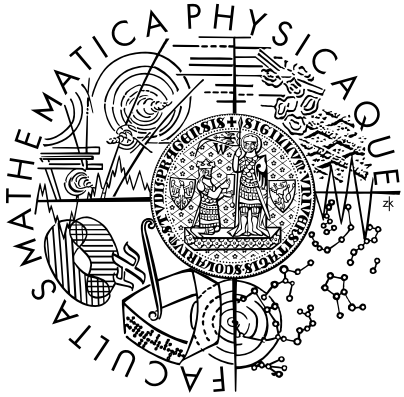

Prague, 2010

Univerzita Karlova v Praze
Matematicko-fyzikální fakulta
Katedra geofyziky

Autoreferát doktorské disertační práce

Numerické modelování dynamiky pevninských ledovců

Ondřej Souček

Školitel: prof. RNDr. **Zdeněk Martinec**, DrSc.

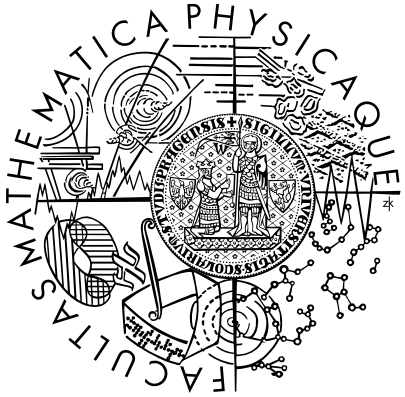

Praha, 2010

Výsledky disertační práce byly získány během prezenčního doktorského studia na Katedře geofyziky MFF UK v Praze v letech 2005 až 2010.

Uchazeč:
RNDr. Ondřej Souček
Katedra geofyziky MFF UK
V Holešovičkách 2
180 00, Praha 8

Školitel:
prof. RNDr. Zdeněk Martinec, DrSc.
Katedra geofyziky MFF UK
V Holešovičkách 2
180 00, Praha 8

Školící pracoviště:
Katedra geofyziky MFF UK
V Holešovičkách 2
180 00, Praha 8

Oponenti:

Dr. Erik R. Ivins
Jet Propulsion Laboratory
M/S 300-233
4800 Oak Grove Drive
Pasadena, CA 91109
United States

prof. RNDr. Josef Málek, CSc., DSc.
Matematický ústav UK
Sokolovská 83
186 75, Praha 8
Česká Republika

Předseda oborové rady F-7:
doc. RNDr. Oldřich Novotný, CSc.
Katedra geofyziky MFF UK
V Holešovičkách 2
180 00, Praha 8

Autoreferát byl rozeslán dne 30.4. 2010.

Obhajoba disertace se koná dne 1.6. 2010 v 10 hod. před komisí pro obhajoby doktorských disertačních prací oboru F-7 — Geofyzika v budově MFF UK, Ke Karlovu 3, 121 16 Praha 2, v místnosti č. 105.

S disertací je možno se seznámit na studijním oddělení — doktorské studium MFF UK, Ke Karlovu 3, 121 16 Praha 2.

Contents

1 Introduction

Ice sheets are masses of grounded ice that evolve in regions where climatic conditions allow for the long-term deposition of snow cover. At sufficiently long time scales, due to internal creep, glacier ice behaves as a non-Newtonian fluid. This fact enables us to describe and explain the evolution of ice sheets over such time scales by means of continuum thermomechanics, constructing a nonlinear-fluid model with geometry that is controlled by gravitationally driven creep flow, and by the surface processes of accumulation, ablation and basal sliding.

To study the ice-sheet dynamics various numerical modeling techniques may be employed. Since ice sheets are typically flat, with a vertical-to-horizontal aspect ratio smaller than $1/100$, a scaling approximation utilizing this fact is often adopted in the glaciological community, resulting in the so-called Shallow Ice Approximation (SIA). This approximation allows us to easilly compute the ice-sheet velocity field, induced by gravity, semi-analytically, and thus provides an effective computational tool compared to more accurate but also more time-expensive computational approaches. During the last several years, however, the SIA has been slowly abandoned, as the effects of higher-order dynamics or even the exact solution to the ice-flow problem are looked for, typically, by means of advanced numerical techniques such as finite-elements or spectral methods. The increase of computational demands is, however, enormous compared to the SIA, making it problematic to implement these techniques for large-scale evolutionary ice-sheet models.

We have therefore designed an iterative algorithm capable of successive improvement of the SIA solution towards the exact (so called full-Stokes) solution, while still possessing the SIA's computational effectiveness. After being thoroughly tested, the algorithm was incorporated into a large-scale ice-sheet model, providing an alternative numerical tool between the two mentioned extremes - fast but inaccurate SIA on the one hand and accurate but slow advanced numerical techniques on the other. Our approach provides the SIA solution in regions where it is sufficiently accurate, and enables us to significantly improve the solution in regions where the assumption of "shallowness" becomes violated.

2 Theory

2.1 Continuum thermomechanical model

In terms of macroscopic glaciology, the problem of ice-sheet evolution and flow may be viewed as a thermomechanically coupled gravitationally driven flow of a fluid with a nonlinear viscosity, generally depending on both the strain-rate and temperature. In addition, it is a problem with a free-boundary, that is, the glacier's geometry itself is a part of the sought solution.

The ice rheology is specified by an idealized model of a non-Newtonian incompressible fluid with uniform density where the deviatoric part of the Cauchy stress tensor is given by **Glen's flow law** (e.g. Paterson, 1981):

$$\boldsymbol{\sigma} = 2\eta \boldsymbol{d}, \;\; \eta = \frac{1}{2}\mathcal{A}(T)^{-1/n} d_{II}^{(1-n)/n} \;, \; n = 3 \;,$$

or, inversely,

$$\boldsymbol{d} = \mathcal{A}(T)\sigma_{II}^{n-1}\boldsymbol{\sigma} \;,$$

where d_{II}, σ_{II} are the second invariants of the strain tensor $\boldsymbol{d}$, and the stress deviator $\boldsymbol{\sigma}$, respectively. The temperature dependence of the rate-factor $\mathcal{A}(T)$ is of the Arrhenius type

$$\mathcal{A}(T) = A\exp\left(-\frac{Q}{k_B T}\right) .$$

Under the assumption of the uniform ice density and after applying an appropriate scaling of the field quantities, the field equations to be solved read (Hutter, 1983):

$$\begin{aligned} \mathrm{div}\vec{v} &= 0 , \\ -\mathrm{grad}p \,+\, \mathrm{div}\boldsymbol{\sigma} + \rho\vec{g} &= \vec{0} , \\ \boldsymbol{\sigma} &= 2\eta(d_{II}, T)\boldsymbol{d} , \\ \rho c_v \dot{T} &= \boldsymbol{\sigma} : \boldsymbol{d} + \mathrm{div}(k(T)\mathrm{grad}T) . \end{aligned}$$

These field equations are accompanied by boundary conditions at the upper free surface and at the glacier base, and also by kinematic conditions (Greve, 1997)

$$\frac{\partial F_{s,b}}{\partial t} + \vec{v}\cdot\mathrm{grad}F_{s,b} = a^{s,b} , \tag{1}$$

describing the evolution of the free surfaces (given by implicit equations $F_{s,b} = 0$) as a result of both the ice flow and the accumulation-ablation processes (given by the accumulation-ablation functions $a^{s,b}$).

2.2 Shallow Ice Approximation

The Shallow Ice Approximation (SIA) as given in Baral et al. (2001), is an approximation of the equations governing the ice-flow obtained as a leading-order limit of the perturbation expansion in the flatness parameter ϵ which is defined as a fraction of the typical vertical-to-horizontal scales of the ice-sheet geometry. The equations are first made dimensionless by introducing appropriate scales and dimensionless numbers, then a formal polynomial expansion series of any field variable φ is performed in terms of the flatness ratio ϵ

$$\varphi = \sum_{n=0}^{\infty} \varphi^{(n)} \epsilon^n ,$$

and only leading-order form of the final equations is kept, reflecting the fact that typically in nature, the value ϵ is small (typically varying between 10^{-3}-10^{-2} for large ice sheets), thus allowing for such a perturbation procedure.

Traditionally, the SIA is considered in Cartesian coordinates, however, for large-scale modeling, it is appropriate to use more general coordinates, such as spherical, polar or orthographic. To avoid multiple derivations for each particular case, we derived the SIA in general orthogonal curvilinear coordinates. Performing generalisations of the scaling procedure for Cartesian coordinates, we obtain a whole class of SIAs, whose particular realization is given only by evaluating geometrical quantities related to the chosen coordinate system.

The most important feature of the SIA is the applied scaling of the stress tensor components which obey the following hierarchy. The dominant stress is the hydrostatic pressure p. One

order of magnitude smaller in the flatness scaling parameter ϵ are the vertical shear stresses $\boldsymbol{\sigma}_{xz}$, $\boldsymbol{\sigma}_{yz}$ and two orders of magnitude smaller in ϵ are the remaining stress tensor components, the longitudinal stresses $\boldsymbol{\sigma}_{xx}$, $\boldsymbol{\sigma}_{yy}$, $\boldsymbol{\sigma}_{zz}$, and the horizontal shear stress $\boldsymbol{\sigma}_{xy}$. This fact, when employed in the SIA perturbation procedure, allows us to resolve the mechanical part of the ice-flow problem semi-explicitly, namely for a simple Cartesian setting the horizontal components of the velocity field $\vec{v}_H := (v_x, v_y)$ can be derived as

$$\vec{v}_H(x,y,z) = -(\mathrm{grad}_H f_s)\, \mathcal{F}(\|\mathrm{grad}_{\mathrm{H}} f_s\|) \int_{f_b}^{z} \mathcal{A}(T)(f_s - z')^3\, dz' \,,$$

where $\mathrm{grad}_H := (\frac{\partial}{\partial x}, \frac{\partial}{\partial y})$ and f_s is the function describing the elevation of the upper free surface. The vertical component of velocity is then easily obtained from the divergence-free condition. It is crucial from the numerical point of view that the numerical effort necessary to evaluate the above formula is several orders of magnitude smaller compared to the numerical complexity of the original problem.

For a realistic ice-sheet, the SIA approach, however, fails in many regions. Namely close to the ice margin where the typically steep slopes of the ice-sheet surface would in the SIA produce unrealistically high deformational velocities, or e.g. in the so-called ice streams, in regions where basal sliding becomes dominant over the deformational flow and the SIA assumptions are no longer valid as the longitudinal stresses become important or even dominant over the vertical shear stresses.

2.3 Iterative improvement of the SIA solution - the SIA-I algorithm.

To overcome the difficulties with the inherent inaccuracy of the SIA, aware of the extreme increase of computational costs when the SIA is abandoned, we designed an iterative algorithm that successively improves the SIA solution (Souček & Martinec, 2008). The iterations start with the SIA-based stress and velocity fields, which are then updated by solving an approximate problem that has more convenient numerical properties compared to the original setting. The derivation is based on the idea of applying the SIA assumptions not on the whole stress tensor but rather only on the correction increments. One of the main results are the following formulae for the increments of principal stresses δp, $\delta\boldsymbol{\sigma}_{xz}$, $\delta\boldsymbol{\sigma}_{yz}$:

$$\begin{aligned}
\delta p(\cdot,z) &= -p(\cdot,z) - \boldsymbol{\sigma}_{xx}(\cdot,z) - \boldsymbol{\sigma}_{yy}(\cdot,z) + (f_s(\cdot) - z) \\
&- \epsilon\frac{\partial}{\partial x}\int_z^{f_s(\cdot)} \boldsymbol{\sigma}_{xz}(\cdot,z')dz' - \epsilon\frac{\partial}{\partial y}\int_z^{f_s(\cdot)} \boldsymbol{\sigma}_{yz}(\cdot,z')dz' \\
&+ \epsilon\boldsymbol{\sigma}_{xz}(\cdot,f_s(\cdot))\frac{\partial f_s(\cdot)}{\partial x} + \epsilon\boldsymbol{\sigma}_{yz}(\cdot,f_s(\cdot))\frac{\partial f_s(\cdot)}{\partial y}\,, \\
\delta\boldsymbol{\sigma}_{xz}(\cdot,z) &= -\boldsymbol{\sigma}_{xz}(\cdot,z) - \epsilon\frac{\partial f_s(\cdot)}{\partial x}(f_s(\cdot) - z) + 2\epsilon\frac{\partial}{\partial x}\int_{\tilde{z}}^{\tilde{f}_s} \boldsymbol{\sigma}_{xx}(\cdot,z')dz' \\
&+ \epsilon\frac{\partial}{\partial y}\int_{\tilde{z}}^{\tilde{f}_s} \boldsymbol{\sigma}_{xy}(\cdot,z')dz' + \epsilon\frac{\partial}{\partial x}\int_{\tilde{z}}^{\tilde{f}_s} \boldsymbol{\sigma}_{yy}(\cdot,z')dz'\,,
\end{aligned}$$

$$\begin{aligned}\delta\boldsymbol{\sigma}_{yz}(\cdot,z) &= -\boldsymbol{\sigma}_{yz}(\cdot,z) - \epsilon\frac{\partial f_s(\cdot)}{\partial y}(f_s(\cdot)-z) + \epsilon\frac{\partial}{\partial y}\int_{\tilde{z}}^{\tilde{f}_s}\boldsymbol{\sigma}_{xx}(\cdot,z')dz' \\ &+ \epsilon\frac{\partial}{\partial x}\int_{\tilde{z}}^{\tilde{f}_s}\boldsymbol{\sigma}_{xy}(\cdot,z')dz' + 2\epsilon\frac{\partial}{\partial y}\int_{\tilde{z}}^{\tilde{f}_s}\boldsymbol{\sigma}_{yy}(\cdot,z')dz' \ ,\end{aligned}$$

where $(\cdot)$ stands for the pair (x,y) for brevity. By these formulae, we define stress increments in the first half-step of the iterative procedure which we call the **SIA-I**. In its second half step, the updated stress field is forced to better consistency with the rheology by applying the forward and inverse rheological relations.

The proposed iterative procedure, though not as straightforward as the SIA, still possesses the basic features of the original SIA setting. Most importantly its locality, since all the necessary numerical operations consist of only evaluating the horizontal spatial derivatives of the field quantities and one-dimensional integration, both being computationally rather cheap. This implies that the improvement provided by the SIA-I algorithm is numerically effective and fast. A deeper mathematical analysis of the properties of the SIA-I mapping has not been fully achieved yet, our conclusions regarding its the performance mainly follow from the extensive numerical testing.

3 Results - steady-state experiments

3.1 ISMIP-HOM benchmark

With a simple numerical implementation of the SIA-I approach we participated in the **Ice-Sheet Model Intercomparison Project – Higher Order Models (ISMIP-HOM)** (Pattyn, 2007, http://homepages.ulb.ac.be/ ∼fpattyn/ismip/). This benchmark experiment aimed to demonstrate the effects of higher-order solutions of various ice-flow model problems compared to the solution by the SIA, where by "higher-order" all such solutions are meant that take into account the longitudinal stresses.

Our approach has been incorporated into experiments A and B (model *oso1*, see Pattyn et al. (2008)). We also performed the experiment C, where basal sliding with a prescribed sliding law is considered in contrast to A and B where no-slip was considered at the glacier base.

ISMIP-HOM experiment A

This experiment involves a Stokes flow problem with no slip at the bed, stress-free conditions at the surface and the ice is considered isothermal. Realistic values of the physical parameters for ice are considered. The glacier has a square base, the upper surface is inclined and flat whilst the glacier base contains sinusoidal bumps. At the sides, the periodic boundary conditions are prescribed. For various aspect ratios ϵ the surface velocities and basal shear stresses are computed and compared at a specified intersection. In Fig. 1 we display an example of the benchmark output, a comparison of the surface velocities v_x along a given profile, for aspect ratios $\frac{1}{10}$ (left) and $\frac{1}{40}$ (right). Our solution (light blue dots) is compared with other full-Stokes solutions (plotted with lines), and several higher-order models (dots) as published in Pattyn et al. (2008).

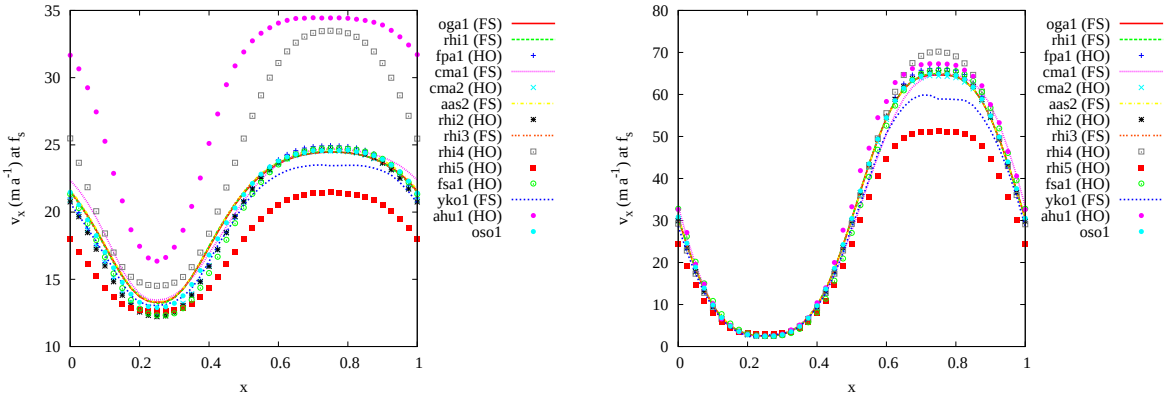

Figure 1: Surface velocities v_x from ISMIP-HOM experiment A, for $\epsilon = \frac{1}{10}$ (left) and $\epsilon = \frac{1}{40}$ (right).

ISMIP-HOM experiment C

The problem is set up very similarly to experiment A, the difference being that the driving effect is, instead of bed-geometry undulations, the spatial inhomogeneity in the basal-friction coefficient. At the glacier bed, the sliding law is prescribed in the form

$$\beta^2 \vec{t}_b \cdot \vec{v} = -\vec{t}_b \cdot \boldsymbol{\sigma} \cdot \vec{n}_b \ ,$$

where $\vec{t}_b$ and $\vec{n}_b$ are the tangent and downward normal vectors to the glacier base f_b, respectively. The sliding coefficient β^2 has sinusoidal pattern in both horizontal directions. The SIA-I algorithm was successfully adopted also for this situation and a good convergence was observed unless a region with strictly zero sliding (free-slip) is present.

Numerical performance

The essential feature of the presented SIA-I approach is its computational effectiveness. The algorithm is designed such that the time cost spent at each iterative step is similar to that required for the SIA approach. Using an Intel Pentium 4, 3.2GHz computer, we have performed 50 iterations for the ISMIP-HOM A setting with $\epsilon = \frac{1}{80}$, which is a sufficient number of iterations so that the SIA-I solution converges. The computational time increases linearly with the increasing number of degrees of freedom. Considering the CPU-time demands for the professionally optimized finite-element solver Elmer (Gagliardini and Zwinger, 2008), for the current ISMIP-HOM A setting the authors provide an analytical formula for CPU-time costs in (s) as a function of the number of degrees of freedom: $y = 0.013x^{1.11}$. Making a similar estimate for the SIA-I solver, we obtain $y = 0.00015x$, which represents a significant speed-up.

3.2 Dronning Maud Land simulation

Thanks to Dr. Oleg Rybak (AWI) and Prof. Dr. Philippe Huybrechts (Vrije Universiteit Brussel), we could perform a test of the SIA-I algorithm on more realistic data. We obtained surface velocities resulting from a higher-order model (Pattyn, 2003) of a 600×400 km region in

Dronning Maud Land, Antarctica. We were also provided with the 3-D temperature field for the whole computational domain. Hence, we can also incorporate the temperature dependence of ice viscosity, which is quite strong, in total, the temperature contribution to the viscosity variation reaches 3 orders of magnitude.

We solve a Stokes-flow problem looking for a steady-state solution with non-homogeneous boundary conditions on velocity at the base, and free-surface conditions at the upper surface. In Fig. 2, we compare the surface deformational velocities from the SIA-I solution (SIA-I), the 2nd-order model by Pattyn (2003) (HOM) and also the solution corresponding to the Shallow Ice Approximation (SIA). We may observe a relatively good agreement between the higher-order model (HOM) and our solution (SIA-I), and a distinct difference between these solutions and the much less smooth result coming from the SIA solution. Concerning the numerical performance, the displayed SIA-I output was obtained after 60 iterations with approximately 3.8 s of CPU time per iteration (performed on an Intel Pentium Core 2 Quad 2.4 x 4, 8GB RAM, 800 MHz, in non-parallel version), while the HOM model took approximately 5000 CPU seconds (on a NEC SX8 in parallel mode using OMP and 8 CPUs, Rybak, pers. comm.).

3.3 Summary

The new iterative SIA-I algorithm is derived on the basis of the traditional scaling "shallow-ice" approach by assuming that the aspect ratio of the vertical/horizontal dimensions of a glacier is sufficiently small. The algorithm represents an iterative extension of the SIA approach, and, in general, may provide an improved solution of the ice-flow problem. The key parameter controlling the performance of the algorithm is the aspect ratio ϵ. For the model examples taken from the ISMIP-HOM A experiment with $\epsilon \leq \frac{1}{10}$, the SIA-I algorithm converges, the case with $\epsilon = \frac{1}{10}$ is however a threshold above which the SIA-I algorithm fails.

The relative simplicity of the SIA-I leads to a computational effectiveness, since the numerical computations consist of only numerical integration over the vertical coordinate and the spatial differentiation of field quantities, which are similar numerical operations as performed in the SIA approach. Moreover, the computational demand grows only linearly with the number of degrees of freedom.

The performance of the SIA-I algorithm was also tested for the ISMIP-HOM experiment C, where a Newton-type sliding law is applied at the glacier base. The SIA-I approach requires the reformulation of the sliding law as a Dirichlet boundary condition for velocity. This disables us to resolve the velocities correctly in the regions with a small sliding friction coefficient β and fails completely for free-slip conditions (β = 0). However, the errors in the velocities are localized in the vicinity of the singular region where $\beta = 0$. The erroneous behavior of the SIA-I algorithm disappears with decreasing aspect ratio. For instance, in the case where $\epsilon = \frac{1}{80}$, the SIA-I converges everywhere in the solution domain and shows good agreement with the published numerical full-Stokes solution.

We also performed a test of the SIA-I approach on more realistic data from Dronning Maud Land, Antarctica, which is a Stokes-flow problem characterized by strongly inhomogeneous Dirichlet boundary conditions for velocity and the temperature dependence of ice viscosity. The comparison with output from a higher-order model again shows a satisfactory performance of the SIA-I algorithm, both in accuracy and computational effectiveness.

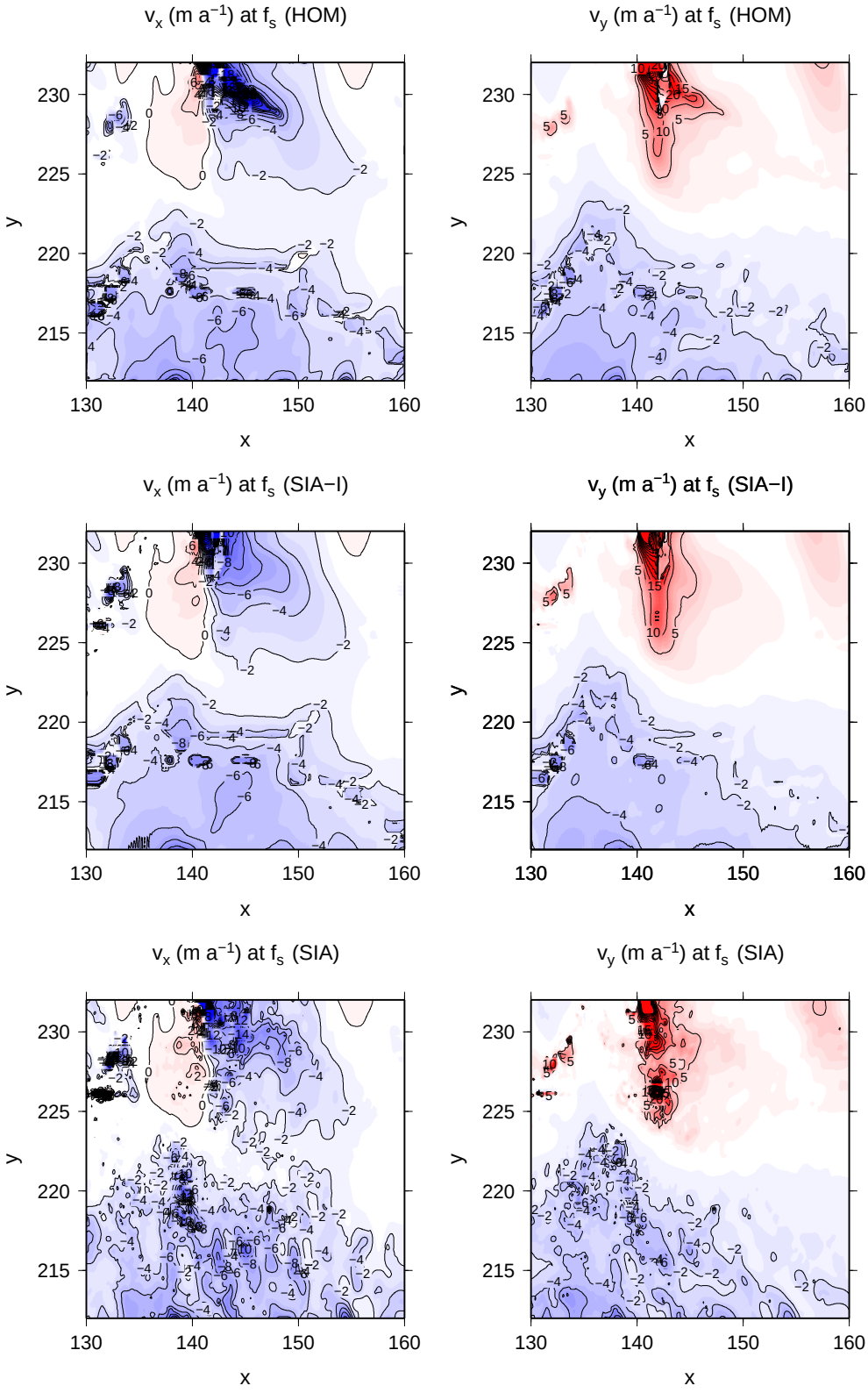

Figure 2: Results of the Dronning Maude Land simulation, deformational surface velocities from the higher-order model (top), SIA-I (middle) and the SIA (bottom).

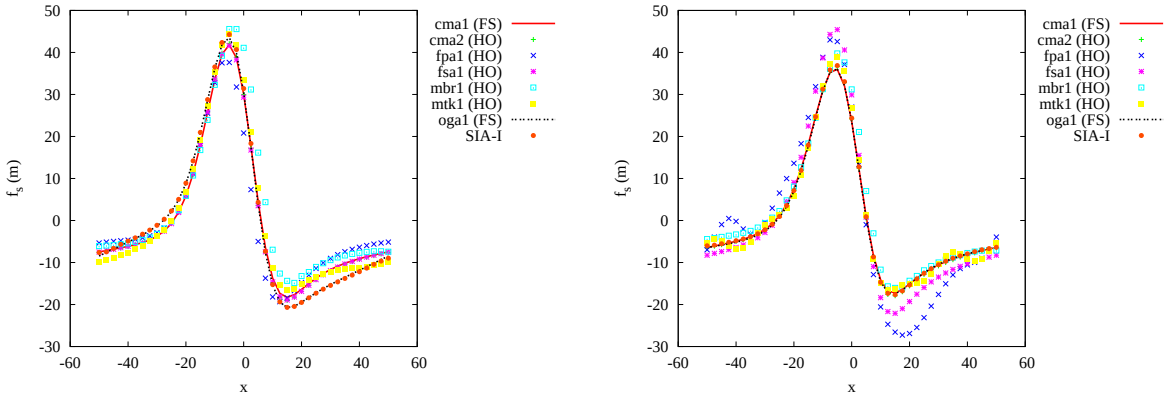

Figure 3: The steady-state geometry profiles for the ISMIP-HOM experiment F, without (left) and with (right) the basal sliding.

4 Results - prognostic experiments

The SIA-I algorithm was implemented into an evolutionary thermo-mechanically coupled numerical ice-sheet model by incorporating also the kinematic equations for the free-surface evolution and the "shallow" limit of the heat-transport equation. We experimented with various numerical approaches towards the kinematic equations and both time-explicit and time-semi-implicit methods have been implemented, the former introduced with the use of Essentially Non-Oscillatory (ENO) Schemes (Shu, 1998) and higher-order Runge-Kutta method, the latter designed in a SIA-like fashion providing a parabolic kinematic equation. In addition, to allow for more advanced determining and tracking the ice sheet margin, a level-set method has been implemented following Peng et al. (2000).

4.1 ISMIP-HOM experiment F

The setting of the ISMIP-HOM experiment F is as follows (Pattyn, 2008). An ice slab, with an initially flat surface slope of $3°$, is flowing over a parallel inclined bed perturbed by a Gaussian bump. Periodic boundary conditions on velocity are applied at the sides of the computational domain. The flow exponent in rheology is chosen $n = 1$, which corresponds to Newtonian (linear) rheology. Ice is considered isothermal and sliding law is adopted with two possible constant sliding parameters, the first corresponding to no-slip conditions and the second allowing for basal sliding. The steady-state surface geometry and velocities are looked for.

The resultant steady-state geometry profiles are shown in Fig. 3. Our solution (SIA-I - red dots) is compared with the published full-Stokes solutions (lines) and other higher-order solutions (points). Note that the SIA-I solution is systematically closer to the cluster of full-Stokes solutions than the most of the remaining higher-order models.

Numerical performance

The computations for both cases, were performed for a model resolution $60 \times 60 \times 40$ and the solution was considered as steady state when the surface profile had not changed within a specified tolerance (maximal relative change of thickness of 5×10^{-5}) for two successive time

steps. Approximately 200 time-steps (1 step = 1 year) were needed to reach the steady-state. Each step took approximately 3s on an Intel Core i7 Quad-Core 2.6x4GHz. This is considerably faster than the full-Stokes FEM model (oga1 in Fig. 3, where the time costs per time step vary between 2 and 0.5 CPU hours (see Fig. 11 in Gagliardini, 2008).

4.2 Transient simulation with non-linear rheology.

The speed-up achieved by employing the SIA-I algorithm allows us to extend the experimental setting of the ISMIP-HOM experiment F and perform an "ISMIP-HOM - like" experiment also for a more realistic non-linear rheology following the Glen's flow law, which is more appropriate for the description of ice behavior. The model was set up as follows. We chose a geometry similar to the ISMIP-HOM experiment A setting, i.e square-base ice slab of size $\mathrm{L_{sc}} \times \mathrm{L_{sc}}$, $\mathrm{L_{sc}} = 80\,\mathrm{km}$, with an initially flat surface flowing over an inclined parallel bed perturbed by sinusoidal bumps. At the sides, the periodic boundary conditions are prescribed and no-slip and no traction were prescribed at the glacier bed and the upper free surface, respectively. Our model was run until the upper surface was moving not more than a specified tolerance (the same as for the ISMIP-F experiment above). Such a stage, considered as steady state, was reached after approximately 200 time-steps (1 time-step = 1 year). To check our simulations, we implemented this model setting into the open-source finite-element code Elmer (http://www.csc.fi/english/pages/elmer). Since the time demands for the non-linear rheology given by Glen's flow law are too large to run the whole transient simulation, we confined ourselves to compare the SIA-I and full-Stokes FEM solutions only at several time instants. For each of these times we substituted the SIA-I computed geometry into a steady-state finite-element simulation as input data and obtained the corresponding full-Stokes velocity field. This was compared with our SIA-I velocities. The results show a good agreement between the computed velocity fields, indicating that our SIA-I solution of the steady-state surface profile is close to the full-Stokes solution.

The time costs of the SIA-I solver do not differ from the ISMIP-HOM experiment F, that is they are of the order of seconds per a time-step, depend linearly on the model resolution (number of nodes).

4.3 Axisymmetric ice-sheet spreading

In this numerical experiment, we compute the flow of an axisymmetric ice cap under its own weight. We compare the SIA-I solution for several aspect-ratios with a finite-element transient simulation performed by the Elmer code. The initial shape of the glacier is a spherical cap and aspect ratios $\epsilon = \frac{1}{10}, \frac{1}{20}, \frac{1}{50}, \frac{1}{100}$ are examined. Ice rheology is modelled by Glen's flow law, at the glacier bed a sliding law is prescribed with a constant sliding parameter and the upper surface is taken as traction-free. A satisfactory agreement between the evolutionary finite-element full-Stokes simulation and the SIA-I result was observed even for the largest considered aspect ratio of $\epsilon = \frac{1}{10}$.

4.4 EISMINT benchmarks - effects of thermomechanical coupling

The performance of the heat-equation solver was checked in the comparison with the European Ice Sheet Modeling INiTiative (EISMINT), a series of benchmark experiments designed for testing the role of thermomechanical coupling in the ice-flow problem. Two prognostic equations are solved: (i) the heat-transport equation, and (ii) the free-surface evolution resulting from ice deformation and surface accumulation and ablation. The nonlinear rheology of ice is given by Glen's flow law with the rate factor of the Arrhenius dependence. Ice is assumed to be cold, i.e. its temperature is not allowed to exceed the pressure melting point. For all numerical experiments, the accumulation-ablation function and the surface temperature are prescribed at the free-surface. At the glacier base, the no-slip boundary condition for velocity is assumed and a constant geothermal heat flux is specified. No melting is taken into account, neither at the base, nor inside the glacier. Realistic physical parameters are considered. The bedrock is flat, meaning that the effect of isostasy is not considered. As all the models in the intercomparison are SIA-based models, we perform only the first iteration of the SIA-I algorithm, resulting in the SIA solution.

We performed four experiments A, B, C and D. In experiment A, an equilibrium shape is sought, starting from initially ice-free conditions on a flat bedrock topography when a climatic forcing is specified. The experiments B, C and D are initiated from the steady-state solution (obtained after 200 ky) of experiment A and apply altered temperature or accumulation-ablation conditions. We compare our model output with the published results of the EISMINT benchmark (Payne et al., 2000). The results are summarized in Tables 1–4. Our model is capable of reproducing the results of the EISMINT benchmarks with a sufficient accuracy.

4.5 Greenland Ice Sheet simulation

We applied our numerical model to a realistic simulation. Inspired by the EISMINT intercomparison, in particular by the EISMINT Greenland models benchmark, we have run three different simulations. First, a steady state of the Greenland Ice Sheet (GIS) is sought if the present-day climatic forcing is kept constant during a transient response of the model. The second simulation aims at reconstructing the Greenland Ice Sheet behavior during the last 250 thousand years, i.e. approximately two glacial cycles. The third simulation is a prognostic experiment of modeling a short term (500 years) response of the GIS to a prescribed warming forcing.

4.5.1 Steady-state Greenland Ice Sheet simulation

We perform the EISMINT Greenland Ice Sheet steady-state experiment as described by Huybrechts (1998). The summary of this experimental setup is as follows. The bedrock and surface topography of the Greenland region arew given by a data set compiled by Letreguilly (1991). The accumulation rates on the same grid are provided for the EISMINT experiment by Huybrechts (1998), and are compiled from data by Ohmura & Reeh (1991). The ablation is parametrized by the positive degree-day method (van der Veen, 2007). The model was run for 150 thousand years, with a time step of 5 years, which was sufficiently long to reach the steady-state. We observed that the effect of present climatic forcing mainly influences the coastal regions,

Table 1: EISMINT exp. A results.

Quantity	Our result	EISMINT mean	EISMINT range
Ice volume ($10^6\,\mathrm{km}^3$)	2.074	2.128	0.145
Glaciated area ($10^6\,\mathrm{km}^2$)	1.031	1.034	0.086
Melt fraction	0.582	0.718	0.290
Divide thickness (m)	3710.386	3688.342	96.740
Divide basal temperature (K)	254.538	255.605	2.929

Table 2: Differences between exp B and exp A.

Quantity	Our result	EISMINT mean	EISMINT range
Ice volume change (%)	−2.956	−2.589	1.002
Melt fraction change (%)	12.614	11.836	18.669
Divide thickness change (%)	−5.457	−4.927	1.316
Divide basal temperature change (K)	4.587	4.623	0.518

Table 3: Differences between exp C and exp A.

Quantity	Our result	EISMINT mean	EISMINT range
Ice volume change (%)	−27.884	−28.505	1.204
Glaciated area change (%)	−20.376	−19.515	3.554
Melt fraction change (%)	−21.964	−27.806	31.371
Divide thickness change (%)	−12.678	−12.928	1.501
Divide basal temperature change (K)	3.680	3.707	0.615

Table 4: Differences between exp D and exp A.

Quantity	Our result	EISMINT mean	EISMINT range
Ice volume change (%)	−11.943	−12.085	1.236
Glaciated area change (%)	−10.188	−9.489	3.260
Melt fraction change (%)	−2.309	−1.613	5.745
Divide thickness change (%)	−2.049	−2.181	0.532
Divide basal temperature change (K)	−0.179	−0.188	0.060

where the extent of the GIS is increased. On the other hand, the topography of the Greenland's interior does not change much and slightly decreases the maximum ice thickness.

4.5.2 Climatic cycle experiment

This simulation starts from the steady-state achieved in the first experiment. A climatic forcing for a period of approximately 250 thousand years is imposed, consisting of temperature and sea-level contributions. The temperature changes are derived from the $\delta^{18}O$ content of the GRIP ice core (Dansgaard et al., 1993) by the simple conversion

$$\Delta T\ (\mathrm{K}) = 1.5(\delta^{18}O + 35.27)\ .$$

Sea-level change constrains the maximal extent of the ice sheet, because immediate calving is assumed whenever the ice sheet reaches the ocean (i.e. no ice-shelf formation is considered). It is again correlated directly to the $\delta^{18}O$ content by the formula (Imbrie et al., 1982)

$$\Delta\mathrm{Sea\ level}\ (\mathrm{m}) = -34.83(\delta^{18}O + 1.93)\ .$$

In Fig. 4, we display the surface topography for several snapshots during the last glacial cycle, i.e since approximately 150 thousand years ago, to the present, showing the quite substantial reduction in the GIS extent approximately 125 thousand years ago, which is followed by gradual regrowth of the Greenland Ice Sheet towards the present state - see bottom row in Fig. 4. Our results are in satisfactory agreement with the published benchmark solutions.

4.5.3 Greenhouse warming scenario

This experiment aims at evaluating the effect of one of the possible greenhouse-warming scenarios on the GIS. Started from the steady-state result of the first simulation, the model is run for 500 years into the future, with the climatic forcing based solely on surface temperature increase. Hence, no sea-level forcing is considered. The surface temperature is increased annually by 0.035° C for the first 80 years (total 2.8° C increase) and then by 0.0017° C for the remaining 420 years (0.714° C), resulting in a total temperature increase of 3.514° C after 500 years. This model temperature forcing is based on the proposed scenario by Manabe & Stoufer (1994).

Given the initial and final topography, the topography difference and the evolution of the glaciated area and ice volume are computed, the reduction of the GIS volume is approximately by $0.135 \times 10^6\ \mathrm{km}^3$.

5 Conclusions

We have been dealing with several aspects of the large-scale numerical modeling of ice sheets, both from the theoretical and numerical perspective.

First, we have formulated the equations that govern the time evolution of grounded ice sheets in a form that allows us to capture and incorporate liquid water and estimate the effects induced by its presence, such as an enhanced ice deformation, increased basal sliding caused by lubrication of the bedrock till, thermal effects connected with latent heat release, and so on. Based on the principles of rational mixture thermodynamics, we rederived the traditional Shallow-Ice Approximation, that is a scaling approximation which makes use of the fact that, in nature, the vertical-to-horizontal aspect ratio is often a small number. This fact allows a perturbation analysis in terms of this ratio. Our main contribution is that we have extended the

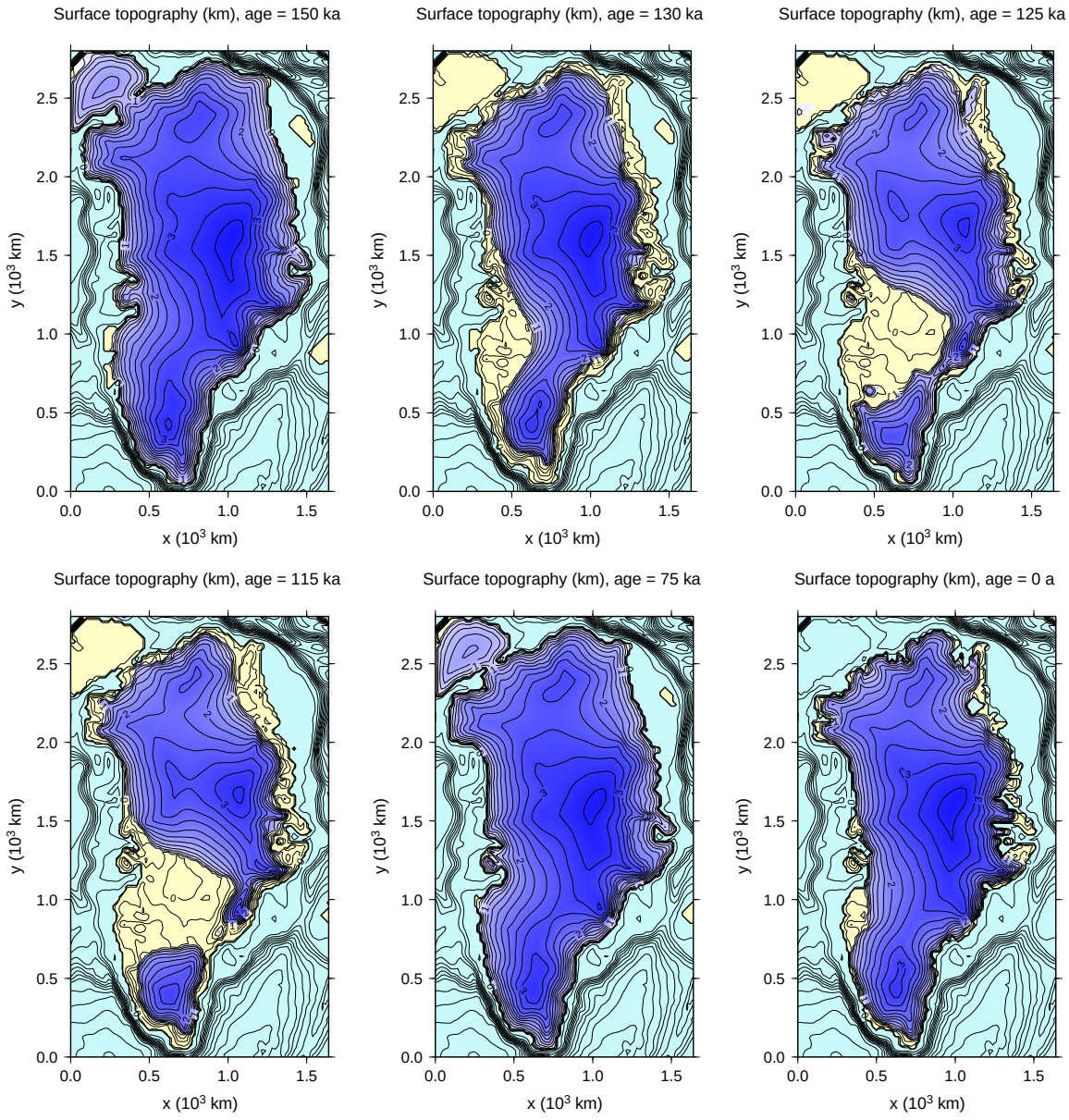

Figure 4: The GIS topography for several snapshots during the climatic cycle experiment.

SIA apparatus by considering general orthogonal curvilinear coordinates and obtained a whole class of SIAs whose particular form depends on the chosen coordinate system, and may be easily specified by evaluating associated geometrical quantities.

We designed a novel computational algorithm denoted as SIA-I, which iteratively improves the "shallow-ice" solution by including longitudinal stresses in a computationally effective way compared to other approaches. The convergence of the algorithm was investigated numerically but also theoretically, leading to the observation that the iterations converge the faster the "shallower" the problem, that is the smaller the scaling parameter ϵ and a threshold value of ϵ seems to exist for each particular setting, above which the algorithm need not converge. Although the rigorous mathematical analysis of the convergence properties of the SIA-I procedure remains to be completed, a number of numerical examples and tests have clearly demonstrated the applicability of the algorithm in practise. We also proved theoretically that if the procedure converges, the limiting solution satisfies the rheological equation exactly and results in errors in the first two momentum equations, that are of the order of ϵ^2 and can be evaluated explicitly.

We performed comprehensive numerical testing by the verification with other numerical methods such as finite-elements, and by computing a number of benchmark examples. We participated in one of the recently designed benchmarks, the Ice-Sheet Model Intercomparison Project - Higher-Order Models (ISMIP-HOM), which was mainly oriented to evaluate the non-shallow, higher-order effects in glacier dynamics. This benchmark reported the good performance of the SIA-I technique, both in accuracy and computational speed.

We also compared our model with a higher-order solution for the region of Dronning Maud Land in Antarctica, by (i) considering realistic topography for both the ice sheet surface and the underlying bedrock surface, (ii) the strongly non-homogeneous basal sliding conditions, and (iii) spatially varying temperature field. The comparison was satisfactory, as the achieved accuracy was comparable with other higher-order models but the results were obtained with a substantially increased computational speed.

We employed the SIA-I technique into a finite-difference thermo-mechanical evolutionary ice sheet numerical model, capable of modeling the evolution of ice sheet geometry due to the processes of internal deformation, described by a model of viscous non-Newtonian fluid, and due to surface processes such as accumulation, ablation and basal sliding. For most simple setups, with only one iteration of the SIA-I algorithm performed at each time step, this model gave similar results to other existing large-scale SIA models such as e.g. SICOPOLIS (http://sicopolis.greveweb.net/), or GRISLI (Ritz et al., 2001). With more than one iterations of the SIA-I algorithm, our model, however, provides (also locally if necessary) an improved solution to the ice-flow problem by capturing the higher-order dynamics by including the longitudinal stresses, which are neglected in the SIA.

The performance of the code was tested for four of the European Ice-Sheet Modelling INiTiative (EISMINT) benchmarks that are focused on the effects of thermo-mechanical coupling within an ice sheet while considering the SIA, with the conclusion that our outputs are in a good agreement with the published results.

We also carried out three benchmarks whose level of complexity fully corresponds to the original purpose of our model, that is, modeling long-term large-scale evolution of large ice sheets. Three EISMINT scenarios of the Greenland Ice Sheet with realistic topographical data, energy and mass fluxes were considered: a steady-state simulation, a paleoclimatic simulation for the period of last two glacial cycles and a 500 year prognostic simulation modeling the

possible effects of a prescribed global-warming prognosis.

6 Acknowledgements

I would first like to thank to my supervisor, Prof. Zdeněk Martinec, for his inspiring leadership and encouragement, to Dr. Ladislav Hanyk, Dr. Jakub Velímský, and Dr. Marie Běhounková, for their advice and often crucial help with the numerical implementations, and to Doc. Ctirad Matyska, for the fruitful discussions and his neverending patience. I am very thankful to Doc. Ondřej Čadek, and Prof. Jan Kostelecký for their support, to Dr. Oleg Rybak and Prof. Philippe Huybrechts for providing their model outputs for the Dronning Maude Land simulation, and last but not least to Dr. Kevin Fleming for his help with the English corrections. I would like to thank sincerely all of the teachers, colleagues and students from the Department of Geophysics, for the unique and friendly atmosphere they created.

The work was supported by the Center for Earth Dynamic Research, and also by the Grant Agency of Charles University in Prague through Grant No. UK/252217.

7 References

Baral, D.R., K. Hutter, R. Greve, 2001. Asymptotic theories of large-scale motion, temperature and moisture distribution in land-based polythermal ice sheets. A critical review and new developments, *Appl. Mech. Rev*. **54**(3), 215–256.

Dansgaard, W., S.J. Johnsen, H.B. Clausenm, D. Dahl-Jensen, N.S. Gunderstrup, C.U. Hammer, C.S. Hvidberg, J.P. Steffensen, A.E. Sveinbjrnsdottir, J. Jouzel, and G. Bond, 1993. Evidence for general instability of past climate from a 250-kyr ice-core record. *Nature* **364**: pp 218-220

Gagliardini, O., T. Zwinger, 2008. The ISMIP-HOM benchmark experiments performed using the Finite-Element code Elmer. *The Cryosphere Discuss.*, **2**, 75-109.

Greve, R., 1997. A continuum-mechanical formulation for shallow polythermal ice sheets, *Phil. Trans. R. Soc. Lond. A* **355** (1726), 921-974.

Hutter, K., 1983. Theoretical Glaciology; material science of ice and the mechanics of glaciers and ice sheets. Reidel, Dordrecht, Netherlands, 510 pp.

Huybrechts, P., 1998. Report of the Third EISMINT Workshop on Model Intercomparison. European Science Foundation (Strasbourg), 120 p.

Imbrie, J., J.D. Hays, D.G. Martinson, A. McIntyre, A.C. Mix, J.J. Morley, N.G. Pisias, W.L. Prell, and N.J. Shackleton, 1982. The orbital theory of Pleistocene climate: Support from a revised chronology of the marine delta18O record. in Berger, A.L. et al. (eds) : Milankovitch and climate, part I, NATO ASI series, p 269-305.

Letreguilly, A., P. Huybrechts, N. Reeh, 1991. Steady state characteristics of the Greenland ice sheet under different climates. *J. glaciol.* **37** (125): pp 149-157

Manabe, S., R.J. Stouffer, 1994. Multiple century response of a coupled oceanatmosphere model to an increase of atmospheric carbon dioxide. *J. Climate*, **7**, 5-23.

Ohmura, A., N. Reeh, 1991. New precipitation and accumulation maps for Greenland. *J. Glaciol.* **37**: pp 140-148.

Paterson, W. S. B., 1981. The Physics of Glaciers. Pergamon Press, Oxford.

Pattyn, F., L. Perichon, A. Aschwanden, B. Breuer, B. de Smedt, O. Gagliardini, G. H. Gudmundsson, R. Hindmarsh, A. Hubbard, J. V. Johnson, T. Kleiner, Y. Konovalov, C. Martin, A. J. Payne, D. Pollard, S. Price, M. Rckamp, F. Saito, O. Souček, S. Sugiyama, and T. Zwinger, T., 2008. Benchmark experiments for higher-order and full Stokes ice sheet models (ISMIP-HOM), *The Cryosphere Discuss.*, **2**, 111-151.

Pattyn, F., 2003. A new three-dimensional higher-order thermomechanical ice-sheet model: basic sensitivity, ice-stream development and ice flow across subglacial lakes. *J. Geophys. Res.* **108**-B8 2382.

Payne, A.J. , Ph. Huybrechts, A. Abe-Ouchi, R. Calov, J.L. Fastook, R. Greve, S.J. Marshall, I. Marsiat, C. Ritz, L. Tarasov, and M.P.A. Thomassen, 2000. Results from the EISMINT model intercomparison: the effects of thermomechanical coupling. *Journal of Glaciology*, 46(153), 227-238.

Peng, D., B. Merriman, S. Osher, H.K. Zhao, and M. Kang, 1999. A PDE based fast local level set method, *J. Comp. Phys.*, 155:410-438.

Ritz, C., V. Rommelaere and C. Dumas, 2001. Modelling the evolution of the Antarctic ice sheet over the last 420 000 years: implications for altitude changes in the Vostok region, *Journal of Geophysical Research*, **109**, 31943-31964.

Shu, C.-W., 1998. Essentially non-oscillatory and weighted essentially non-oscillatory schemes for hyperbolic conservation laws, in Advanced Numerical Approximation of Nonlinear Hyperbolic Equations, edited by A. Quarteroni, Lecture Notes in Mathematics, Springer-Verlag, Berlin/New York, Vol. 1697, p. 325.

Souček O., Z. Martinec, 2008. Iterative improvement of the shallow-ice approximation. *Journal of Glaciology* (1.881), **54**, 188, 812-822.

van der Veen, C.J., 1999. Fundamentals of Glacier Dynamics, A.A. Balkema, Rotterdam, Netherlands, 462 pp.